Progress in Natural Science: Materials International 31 (2021) 898–903

HOSTED BY

Contents lists available at ScienceDirect

Progress in Natural Science: Materials International

journal homepage: www.elsevier.com/locate/pnsmi

Original Research

Mechanical response to axial strain in WS_2 nanotubes

S. Mejía-Rosales [a,*], S.A. Sandoval-Salazar [b], A. Soria-Sánchez [b], J.D. Vázquez-Palafox [b]

[a] Centro de Investigación en Ciencias Físico-Matemáticas (CICFIM), Facultad de Ciencias Físico-Matemáticas, Universidad Autónoma de Nuevo León, San Nicolás de los Garza, N.L, 66455, Mexico

[b] Facultad de Ciencias Físico-Matemáticas, Universidad Autónoma de Nuevo León, San Nicolás de los Garza, N.L, 66455, Mexico

ARTICLE INFO

Keywords:
Tungsten disulfide nanotubes
Young's modulus
Stillinger-weber
Molecular dynamics

ABSTRACT

In order to take advantage of inorganic nanotubes for their use with pragmatic purposes, characterization of their mechanical properties becomes a relevant issue. In the present study, a series of results on the mechanical properties of WS_2 nanotubes of several diameters and two main lattice orientations was obtained by the implementation of molecular dynamics simulations using an interatomic potential of the Stillinger-Weber kind. A Young's modulus for nanotubes of H polytype close to 170 GPa was obtained in accordance with experimental results, and of ≈ 130 GPa for nanotubes of the T polytype, with almost no dependance on the diameter of the nanotube. The tensile strength was as large as 20 GPa (H armchair nanotubes, close to the value obtained in experiments), and the strain at the point of rupture reached values close to 0.24. The effect of several kinds of defects on the mechanical properties was investigated, and the results showed that when the defects consisted in the absence of a whole WS_2 unit, the tensile strength and point of rupture dropped considerably, and the fracture became more brittle than in pristine nanotubes. The dependence of the mechanical properties on temperature was also investigated.

1. Introduction

Since their discovery by the group of Tenne [1], inorganic nanotubes have allowed a broad expanse of potential applications of one-dimensional materials. Transition metal dichalcogenides with general formula TX_2 (where T is a transition metal), such as MoS_2 and WS_2, can be grown in two-dimensional layers just as graphite, and the layers may fold into themselves to form nanotubes. Currently, WS_2 nanotubes of several μm of length can be prepared in fair amounts using relatively simple methods [2–4]. While the tubular structure of these materials is somewhat similar to the structure of carbon nanotubes, transition metal dichalcogenide nanotubes exhibit different mechanical and electronic properties. The characterization of the mechanical properties of these nanostructures thus becomes a critical issue for their exploitation in practical applications. The degree of control required for the measurement of mechanical properties of these nanostructures is challenging, but there have been great advances in this matter in the last years [3]. It is known by nanomechanical measurements that WS_2 nanotubes have a very high strength at the point of fracture [5], and a Young's modulus close to 171 GPa [6]. Mechanical properties are inherently related to electronic properties in transition metal dichalcogenides since the band gap of a monolayer can be tuned by applying mechanical strain; it has been found that by compression or tension of a WS_2 monolayer the bandgap can be modulated, and it can be changed from direct (at strain 0) to indirect [7].

As it is widely known, transition metal dichalcogenides, including WS_2, grow as layers formed by a central metal sublayer confined between two chalcogen—namely, S—sublayers. As a three-dimensional material the layers are kept together by weak van Der Waals interactions. Three main polytypes exist for three-dimensional WS_2, each differing from the others in the relative positions of the two S atoms with respect to the W atom in a WS_2 unit, and in the stacking sequence of the layers. In the 1T polytype, the metal atoms have octahedral coordination, with the S–W–S units forming diagonal patterns, whereas in the 2H and 3R polytype the coordination of the metal atoms is trigonal-prismatic, and the pattern formed takes a chevron shape [8]. The unit cell of the 3R polytype requires the presence of three layers, and thus it is out of the scope of this work. There exist metastable phases, also out of the scope of this work, obtained by the distortion of 1T structures, such as the monoclinic 1T′ and the orthorhombic Td phases, while tetramerization within the transition metal sublattice produces a 1T″ phase, and trimerization produces a 1T‴ phase [9]. This work is centered on monolayers with the

* Corresponding author.
E-mail address: sergio.mejiars@uanl.edu.mx (S. Mejía-Rosales).

https://doi.org/10.1016/j.pnsc.2021.11.004
Received 15 September 2021; Received in revised form 5 November 2021; Accepted 11 November 2021
Available online 8 December 2021

coordination of the 1T and 2H phases. For the structures of just one layer, the numbers appearing in the identification of the polytypes are unnecessary, and we will refer to them simply as T (octahedral coordination) and H (trigonal-prismatic coordination). When one of these layers is bent onto itself, a nanotube forms, and the way the nanotube can be rolled up depends on the orientation of the lattice with respect to the main axis of the tube. Just like in the case of carbon nanotubes, the indices (n,m) that define the chiral vector $\overrightarrow{c} = n\overrightarrow{a_1} + m\overrightarrow{a_2}$ are used to identify the type of a nanotube [10]: when the indices are $(n,0)$ the nanotube is zigzag; if the indices are (n,n), the nanotube is armchair. Other indices (n,m) give chiral nanotubes.

In an authors previous work the mechanical properties of MoS_2 nanotubes covering a range of diameters and temperatures has been investigated [11]. In this work a set of molecular dynamics simulations of the uniaxial stress of WS_2 nanotubes of the T and H polytypes are performed, with armchair and zigzag lattice orientations. The stress-strain curves are obtained, the Young's modulus for each nanotube measured, and the effect of both temperature and the presence of defects on the atomistic arrange in the mechanical properties of the nanotubes investigated. In what follows the simulation setup and the interactions used to model the atomistic interactions are described.

2. Methods

The models of armchair and zigzag WS_2 nanotubes were built, with the diameters varying from 30 to 100 Å, and the lengths of approximately 100 Å. The number of atoms in a nanotube segment inside the simulation box, reported on Table 1, depends on the kind and diameter of the nanotube. The nanotubes were positioned inside the simulation box using periodic conditions in the direction of their main axes. In order to investigate the effects of defects, besides the pristine nanotubes, nanotubes with one of four possible defects on the atomistic arrangements were also prepared. And the four types of the defects are as follows:

Table 1
Lattice orientation, diameter, number of atoms per segment, and (n,m) indices of the WS_2 nanotubes considered for the tensile stress simulations.

Polytype	Orientation	Diameter (Å)	Number of atoms	(n,m)
H	Armchair	29.3	3264	(17, 17)
H	Armchair	39.7	4416	(23, 23)
H	Armchair	48.3	5376	(28, 28)
H	Armchair	58.7	6528	(34, 34)
H	Armchair	69.0	7680	(40, 40)
H	Armchair	79.4	8832	(46, 46)
H	Armchair	89.7	9984	(52, 52)
H	Armchair	98.4	10,944	(57, 57)
H	Zigzag	29.9	3420	(30, 0)
H	Zigzag	39.9	4560	(40, 0)
H	Zigzag	49.8	5700	(50, 0)
H	Zigzag	59.8	6840	(60, 0)
H	Zigzag	69.7	7980	(70, 0)
H	Zigzag	79.7	9120	(80, 0)
H	Zigzag	89.7	10,260	(90, 0)
H	Zigzag	99.6	11,400	(100, 0)
T	Armchair	29.9	3264	(17, 17)
T	Armchair	38.7	4424	(22, 22)
T	Armchair	49.3	5376	(28, 28)
T	Armchair	59.8	6528	(34, 34)
T	Armchair	68.6	7488	(39, 39)
T	Armchair	79.2	8640	(45, 45)
T	Armchair	89.7	9792	(51, 51)
T	Armchair	98.5	10,752	(56, 56)
T	Zigzag	28.4	3024	(28, 0)
T	Zigzag	38.6	4104	(38, 0)
T	Zigzag	48.8	5184	(48, 0)
T	Zigzag	58.9	6264	(58, 0)
T	Zigzag	69.1	7344	(68, 0)
T	Zigzag	79.2	8424	(78, 0)
T	Zigzag	89.4	9504	(88, 0)
T	Zigzag	99.5	10,584	(98, 0)

absence of a whole WS_2 unit (which we called defect of type 1) absence of a W atom (defect of type 2) absence of a S atom from the external sublayer (defect of type 3) and absence of a S atom from the internal sublayer (defect of type 4.) At the length of the nanotubes in the simulation box, the ratios of defects against number of W atoms were from 2×10^{-4} for the widest nanotubes to 3×10^{-4} for the narrowest ones. Prior to the stress simulation the structures were relaxed by a NPT run of 100,000 steps (using a time step of 0.001 ps, a Nosé-Hoover thermostat for temperature control with a damping parameter of 0.1ps, and a Nosé-Hoover barostat with a damping parameter of 1ps) at the temperature at which the nanotubes would be subjected to stress, in order to allow the nanotubes to reach their optimal lengths and diameters. The model for the atomistic interactions is a simplification of the Stillinger-Weber potential [12].

$$V_{SW} = \sum_{j<i} V_2(i,j) + \sum_{i<j<k} V_3(i,j,k)\ ; \tag{1}$$

in this equation, V_2 is a pairwise interaction between atoms i and j of the form

$$V_2(i,j) = C_{ij} e^{\left[\sigma_{ij}/\left(r_{ij}-r_{max_{ij}}\right)\right]} \left(D_{ij}\ /\ r_{ij}^4 - 1\right)\ , \tag{2}$$

while V_3 accounts for the three-body interaction between atoms i, j, and k, such that

$$V_3(i,j,k) = K_{ijk} e^{\left[\sigma_{ij}/\left(r_{ij}-r_{max_{ij}}\right)+\sigma_{ik}/\left(r_{ik}-r_{max_{ik}}\right)\right]} \left(cos\theta_{ijk} - cos\theta_{0_{ijk}}\right)^2\ . \tag{3}$$

The energetic parameters C_{ij} and K_{ij} control the strength of the pairwise and three-body interactions, respectively, while σ_{ij} defines the range of the interaction; D_{ij} has units of r^4, and $r_{max_{ij}}$ and $\theta_{0_{ijk}}$ are the distance and angle cutoffs, respectively. The values of these parameters adjusted by Jiang [13,14] in a study where the obtained phonon spectrum and mechanical properties of WS_2 monolayers reproduced known results; the specific selection of the functional form of the Stillinger-Weber potential was made in order to take into consideration nonlinear effects, while keeping the definition of the potential simple and computationally efficient.

The strain process was simulated using the LAMMPS code [15], imposing a strain rate of $10^9\ s^{-1}$ in the direction of the nanotube's main axis, until reaching a strain enough for the nanotube to break, which usually was accomplished after 1.5×10^6 time steps. As in the relaxation stage, Nosé-Hoover thermostats and barostats were used for the control of temperature and pressure. To solve the equations of motion for the dynamics of the system, a parallelized version of LAMMPS running on a NVIDIA™graphics processing unit (GPU), which is a low-cost alternative that brings an excellent performance-investment ratio, was used [16]. Along the strain runs, stress and strain energy was stored, and atomistic von Mises stress was calculated through the equation of [17].

$$\sigma_{vm} = \frac{1}{\sqrt{2}}\left[\left(\sigma_{xx}-\sigma_{yy}\right)^2 + \left(\sigma_{yy}-\sigma_{zz}\right)^2 + \left(\sigma_{zz}-\sigma_{xx}\right)^2 + 6\left(\sigma_{xy}^2+\sigma_{xz}^2+\sigma_{yz}^2\right)\right]^{1/2}\ . \tag{4}$$

In Eq. *4*, σ_{ij} are the i,j components of the atomic stresses. The definition of the von Misses stress allowed us to visualize locally the effect of the defects on the stress of the atomistic structure of the nanotubes. Young's modulus was calculated from the derivative of the strain energy U_s with respect to the strain ε:

$$Y = \frac{1}{V_0}\frac{\partial U_s}{\partial \varepsilon}\ , \tag{5}$$

where V_0 is the original volume of the layer that forms the nanotube. In the present study for the calculation of V_0 the nanotube was considered as a cylindrical shell of length z_0 and cross section $\pi\left[\left(r_0+\frac{\delta r}{2}\right)^2 -\right.$

$\left(r_0 - \frac{\delta r}{2}\right)^2\Big]$, where r_0 is the original radial distance to the W sublayer, and δr is the separation between layers in bulk WS_2, which was taken as 7.12 Å. The values of diameter $d_0 = 2r_0$ and indices (n, m) for the nanotubes considered in this study are listed in Table 1. The value of Y was also calculated from the slope of the stress-strain curve in the linear elastic regime ($\varepsilon < 0.02$) with essentially the same results.

3. Results

The first issue easily observed from the stress-strain curves was the highly nonlinear response of the nanotubes in the elastic regime. For small strains (less than $\varepsilon = 0.03$) the stress-strain relation was fairly linear, but for higher strains nonlinear effects dominate, to the point that, close to the tensile stress value, the slope of the curve has fallen to values close to zero. Taking this into consideration the Young's modulus only considering values of strain below 0.02 was calculated. Fig. 1 shows a typical engineering stress-strain curve, in this case for an armchair nanotube of the polytype H of approximately 60 Å of original diameter. The curve was obtained at 1 K, but for higher temperatures the behavior of the curve in the elastic regime was similar, with little effect of temperature in the Young's modulus, as will be shown later. Fig. 1 also shows the plot of the strain energy U_s as function of strain, and it can be noted that close to the breakage of the nanotube, the strain energy U_s had a behavior basically linear, and thus stress had quadratic nature. The parametrization of the Stillinger-Weber potential used in the simulations appropriately considers the nonlinear elastic response. The nonlinear elastic constant D, obtained from $\sigma = Y\varepsilon + \frac{1}{2}D\varepsilon^2$, gives $D = -726$ GPa for the armchair H nanotube, and $D = -782$ GPa for the zigzag H nanotube; the nonlinear effect is even greater in nanotubes of the T polytype: $D = -822$ GPa for the armchair, and $D = -918$ GPa for the zigzag. The Poisson's ratio of the H armchair nanotube, calculated using the variation in radius of the nanotube, is $\nu = 0.19$, compared against the value of 0.22 calculated for planar WS_2 layers using density functional theory [18].

Fig. 1 also shows the representation of the segments of WS_2 lattice, both at $\varepsilon = 0$ and at a strain close to the breaking point. In the absence of external load, the W–S interatomic distance was $r_{W-S} = 2.39$ Å, close to the breakage of the nanotube, r_{W-S} reached values between 2.59 and 2.64 Å when the bond was aligned with the main axis of the nanotube, while in the transversal direction the values of r_{W-S} was close to 2.38 Å, not very different from the original bond length. On the other hand, the S–W–S angles became highly deformed, from the original value $\theta_{S-W-S} = 82^\circ$ to values close to 98°.

It is expected that the stress distribution in the pristine WS_2 to be homogeneous in the elastic region, which can be noted in the visualization of the von Mises stress shown in Fig. 2, for the H armchair nanotube of 60 Å. Below the elastic limit the distribution of the von Mises stress was uniform, with a greater magnitude at the W sublayer than at the S sublayers. When the strain reached approximately $\varepsilon = 0.25$ (Fig. 2(d)), some bonds get randomly broken, lowering the von Mises stress locally; thereafter, the fractures extended in the structure of the nanotube (Fig. 2(e)), producing the regions with low values of von Mises stress in the vicinity of the fractures, until the whole structure relaxed itself. The behavior of the distribution of the von Mises stress was qualitatively the same at higher temperatures, but local fluctuations made the color representation less clear than at 1 K. The numeric values assigned to the extremes of the color scale in Fig. 2 are only approximated, particularly for S atoms, since we used the van der Waals radius of a W atom for the calculation of atomic volume, needed for the evaluation of the atomistic von Mises stress.

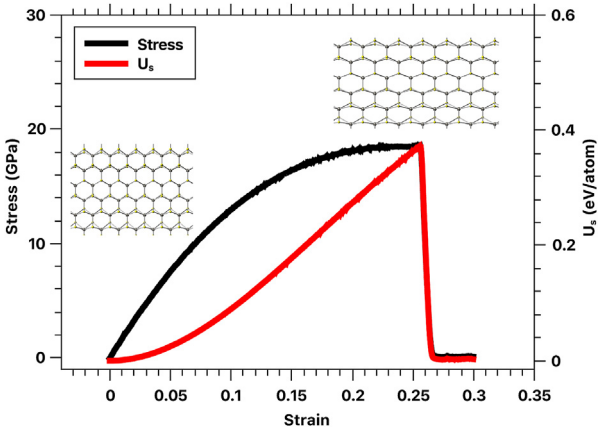

Fig. 1. Stress and strain energy as function of strain, for an armchair nanotube of the H polytype of 60 Å of diameter, at 1 K.

For structures of approximately the same diameter the nanotubes of H polytype had a larger Young's modulus than T polytype nanotubes, as can be noted from Fig. 3, where the values of stress in function of the strain for nanotubes with the diameter of approximately 60 Å was plotted. The trend at other diameters was similar. For a particular polytype, the Young's modulus was not too different between armchair and zigzag nanotubes (in zigzag, Y is usually a few GPa larger that in armchair nanotubes, with the exception of H nanotubes of diameters smaller than 50 Å), but the nonlinear effect was larger in armchair nanotubes. The tensile strength for H nanotubes was significantly larger than for T nanotubes, and accordingly the strain at the point of rupture was larger as well, almost double of that of T nanotubes. The obtained values of the Young's modulus, tensile strength and strain at point of rupture were very close to the ranges obtained experimentally in tensile tests by in situ scanning electron microscopy (SEM), as reported in Ref. [5]. Simulated H nanotubes gave a value of Y between 155 and 170 GPa, which is in very good agreement with Ref. [5] (152 ± 68 GPa), and with measurements using atomic force microscopy, where an average 171 GPa was obtained [6]. Other experiments have produced an average of 162 GPa [19]. The values of Y for the simulated T nanotubes were somewhat lower (around 130 GPa, see Fig. 4), but not very far from those obtained experimentally. In Fig. 3 the representation of measurements made in Ref. [5] were included in order to compare them against the stress-strain curves obtained by the simulations. The representation of measurements on thick, multiwalled WS_2 nanotubes using in situ transmission electron microscopy probing [20] was also included. In these measurements the calculated value of Y was 223 GPa, wich is closer to the value of Y of bulk WS_2 of 272 ± 18 GPa [21].

Polytype H nanotubes presented only a small dependence on diameter of the Young's modulus, while T nanotubes showed a slight tendency of the Young's modulus to decrease at small diameters. This differs from the case of MoS_2 nanotubes, where both polytypes show a small but clear dependency on diameter [11], and occurred at all of the temperatures tested, but it can be noted more clearly for $T = 1K$, as shown in Fig. 4 (a). In comparison, T nanotubes do show a tendency to slightly increase the value of Y with diameter, but this dependency is only significant for diameters smaller than 60 Å. Besides this range of diameters, both the tensile strength and strain at point of rupture appeared to be fairly independent of diameter, as can be noted from Fig. 4 (b) and (c). The independence of the Young's modulus, tensile strength, and point of rupture on diameter makes likely that these results apply even for larger diameters, which is relevant from an experimental standpoint, since typical diameters in experimentally produced WS_2 nanotubes cover a range centered on 150–200 Å [6,22]. The tensile strength in pristine nanotubes is close to fulfill the rule of thumb of 10% the value of Young's modulus [23] (8.5% in H polytype; 12% in T polytype, approximately.)

The effect of the structure defects of the nanotubes on their mechanical properties was investigated. As noted before, four different kind of effects were defined. As can be noted from Fig. 5, the presence of an isolated defect did not have a significant effect on the Young's modulus of the nanotubes, irrespective of the kind of defect, with the exception of T nanotubes of 30 Å of diameter, where it was found that Y actually

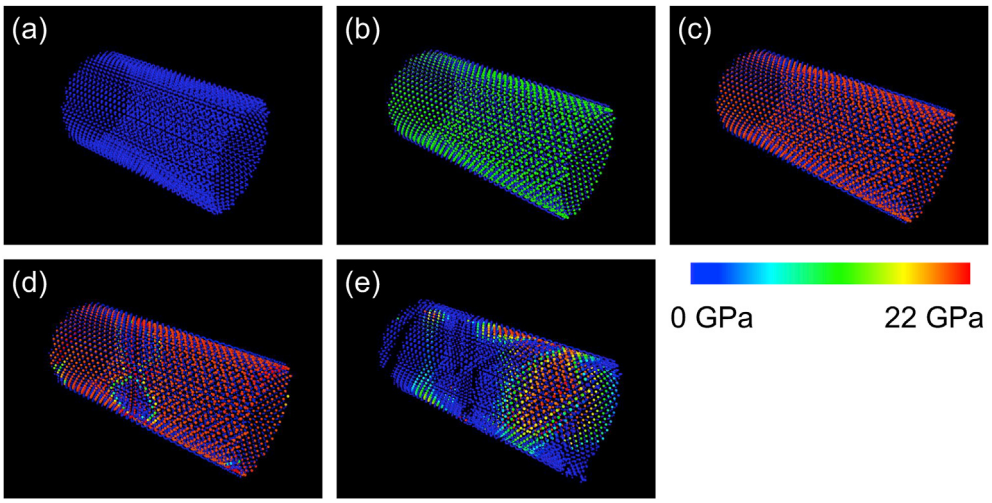

Fig. 2. Von Mises stress distribution at several stages of strain of an H armchair WS_2 nanotube of 60 Å of diameter, at 1 K. a)$\varepsilon = 0$, b)$\varepsilon = 0.09$, c)$\varepsilon = 0.24$, d)$\varepsilon = 0.25$, e)$\varepsilon = 0.26$. The color scale is approximated.

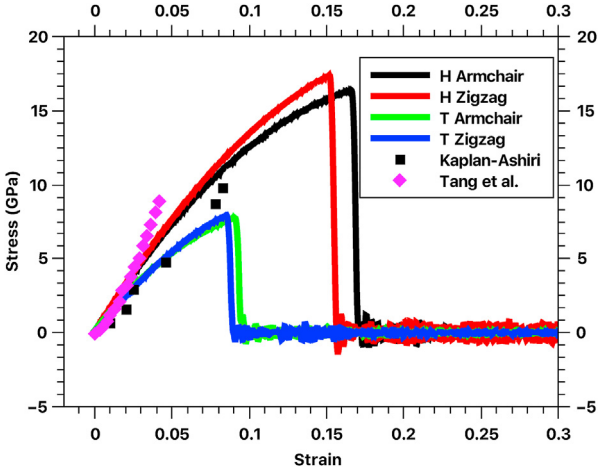

Fig. 3. Stress vs strain relation for WS_2 nanotubes of 60 Å of diameter, at 300 K. Experimental data from Kaplan-Ashiri et al.5 and Tang et al.20.

increases when a defect that considers the absence of a W atom was inserted (defects of kind 1 and 2). Studies on graphene reveal that a low concentration of vacancies may increase the value of the elastic modulus [24,25], and in our case it is likely that local relaxation of the distances between S atoms from distinct WS_2 units due to the presence of the defect may be relevant in the increase of Y when the curvature of the nanotubes is pronounced, but in order to determine the specific role of the presence of defects in this increase additional simulations will be needed to perform in a follow-up work. As it could be expected that the tensile strength and the point of rupture are affected by the presence of the defects, lowering the value of tensile strength by about 4 GPa when either a defect of kind 1 (a whole WS_2 unit) or of kind 2 (a W vacancy) are present, and about 2 GPa with defects of kinds 3 and 4 (external and internal S atoms, respectively). An interest fact about the defects of kind 2, 3 and 4 is that the tensile strength is not affected by the orientation of the WS_2 lattice in both polytypes.

The strain at rupture falls considerably with the presence of defects, which is understandable since a defect acts as a point of concentration of stress where a fracture is eventually developed. This is represented in Fig. 6, where the distribution of the von Mises stress is shown immediately before, during and after the generation of a fracture for a H armchair WS_2 nanotube of 60 Å of diameter, with a defect of the kind 1, at 1 K. In Fig. 6 (a), corresponding to a configuration 8 ps before the fracture starts to propagate, it can be noted that in the region at the vicinity of the defect the von Mises stress falls (blue and green areas), but an X-shaped region centered on the defect is highly stressed; the direction of propagation of this stressed area coincides with the positions of the four hexagons that become incomplete by the subtraction of the WS_2 unit. In Fig. 6 (b), a few W–S bonds at the vicinity of the defect break, the X-shaped region is still highly stressed, and then the fracture starts to propagate lowering the stress (Fig. 6(c) and (d)). The fracture is brittle and very well-defined, following a direction perpendicular to the main axis of the nanotube, at least at the low temperature of 1 K. At a temperature of 300 K the fracture of nanotubes with defects is more ragged, but still following approximately a direction perpendicular to the nanotube's axis, unlike the fracture of pristine nanotubes.

When more than one vacancy is present in the nanotube, which would be a more realistic situation, mechanical properties are strongly affected by the density of defects. When the structures of WS_2 nanotubes with a diameter of approximate 60 Å with several concentrations of vacancies were subjected to tension, the vacancies distributed randomly in the surface of each nanotube. The plots of the Young's modulus vs vacancy percentage are shown in Fig. 7. For comparison two kinds of vacancy

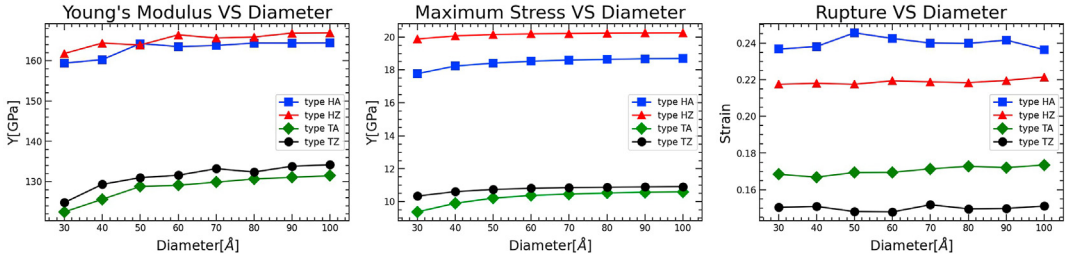

Fig. 4. Dependence of Young's modulus, tensile strength, and point of rupture on the diameter of the nanotube, at 1 K.

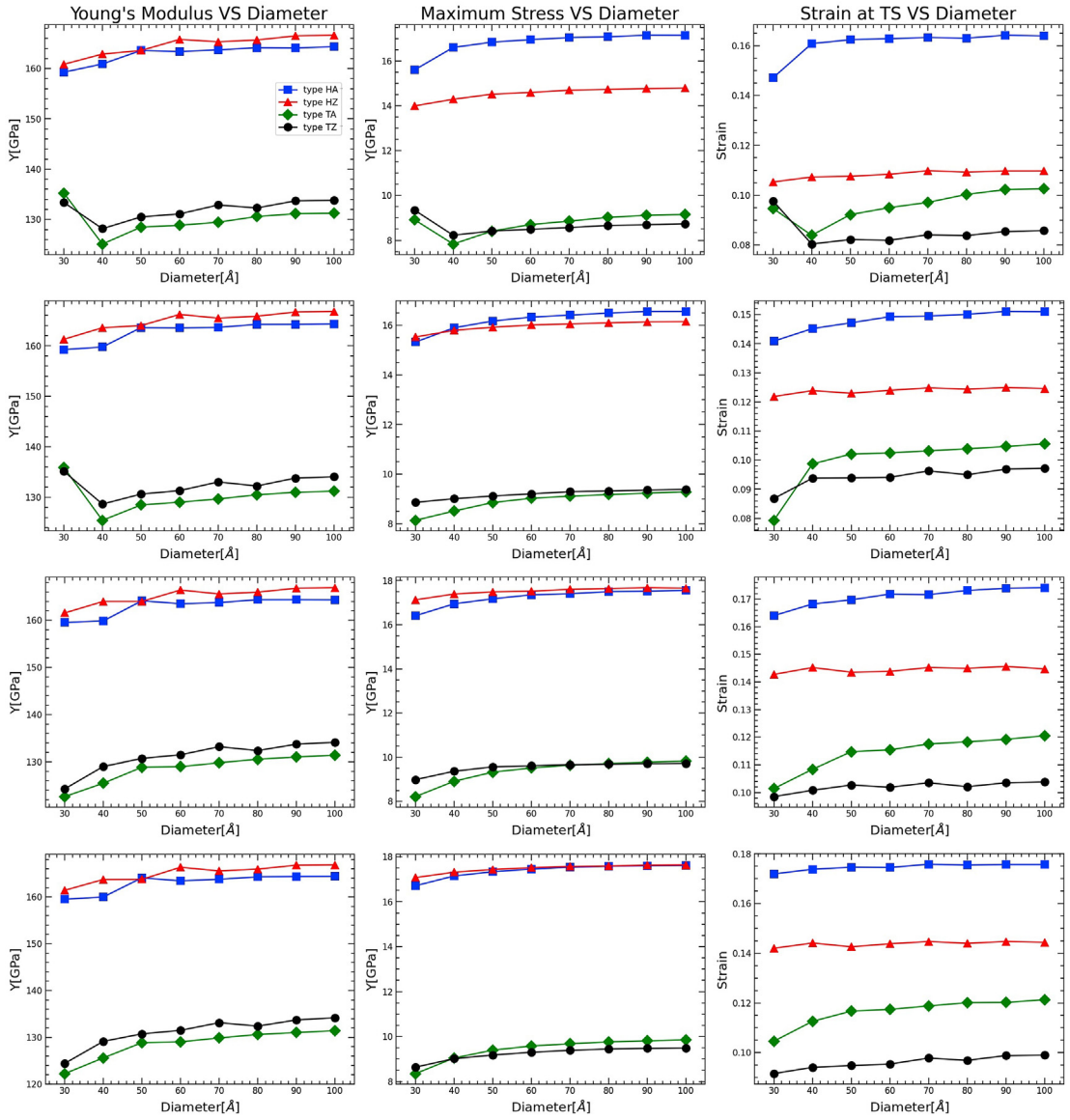

Fig. 5. Dependence of Young's modulus, tensile strength, and point of rupture on the diameter for nanotubes where a defect is inserted, at 1 K. First row: Defect of kind 1; second row: Defect of kind 2; third row: Defect of kind 3; fourth row: Defect of kind 4.

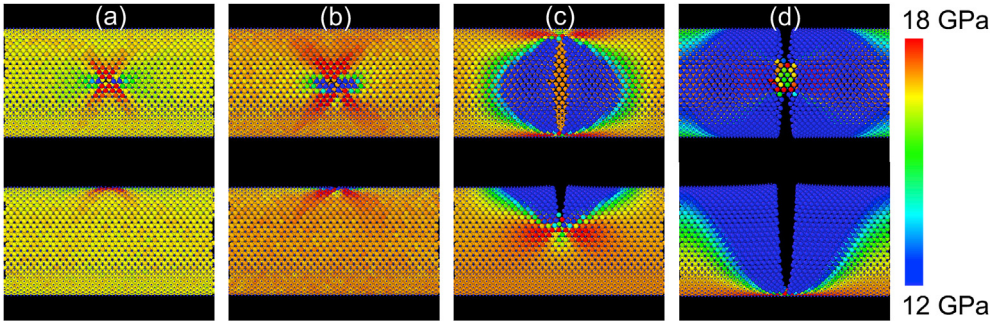

Fig. 6. Frontal (top) and lateral (bottom) views that show the von Mises stress distribution for a H armchair WS_2 nanotube with a defect of the kind 1, at 1 K. a) 8 ps before fracture; b) at the start of the fracture; c) 2 ps after fracture; d) 6 ps after fracture. Color scale is approximated.

defects were used in Fig. 7 defining a vacancy either as the absence of a W atom, or as the absence of a whole WS_2 unit. According to the simulation results, it can be found that the mechanical response was essentially the same disregarding the kind of vacancies present in the structure of the nanotube when the number of vacancies is small. The value of Young's modulus has a linear decay with the percentage of vacancies, at least until

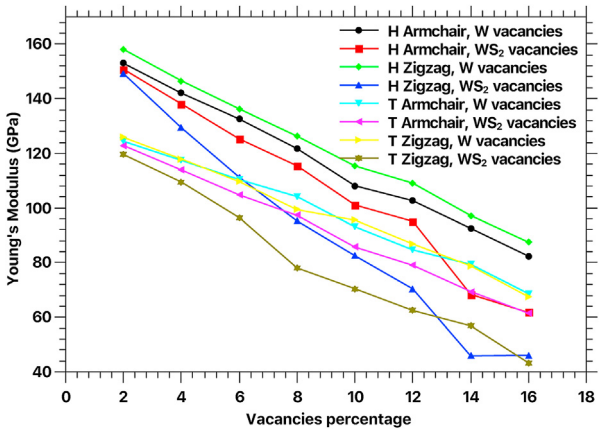

Fig. 7. Young's modulus vs vacancy percentage for WS_2 nanotubes of approximately 60 Å of diameter at 1K, considering either vacancies formed by the absence of a W atoms, or vacancies formed by the absence of a whole WS_2 unit.

reaching a 16% of vacancies (14% for H nanotubes with WS_2 vacancies). For the case of larger percentages the probability of having two or more vacancies as first neighbors in the WS_2 lattice is sufficiently high to make the elastic response dependent on the specific spatial distribution of the vacancies. While the difference in the mechanical response due to the kind of vacancy is only slight for armchair nanotubes when the vacancy percentage is lower than 14%, and in the zigzag nanotubes the Young's modulus gets reduced with the increase of vacancy percentage at a considerably larger rate when the vacancies are missing whole WS_2 units than that when the vacancies are missing only W atoms. Non-linear effects also was reduced as the density of vacancies increased, with the nonlinear elastic constant D reaching values around − 400 GPa in the H nanotubes when the density of vacancies was 16%, and around − 600 GPa for the T nanotubes.

4. Conclusions

Molecular dynamics simulations have been used to study the mechanical properties of WS_2 nanotubes of T and H polytypes, covering a large range of diameters and temperatures. One of the novelties in this study is the use of a recent parametrization of the Stillinger-Weber potential, supported by the reproduction of interatomic angles and distances, and of the phonon spectrum of WS_2 monolayers. This potential is computationally efficient without compromising its precision and stability. The stress-strain relations of a large number of nanotubes for both pristine and including defects on their structure have been established.

For a particular polytype the lattice orientation, temperature, Young's modulus, tensile strength, and point of rupture are slightly dependent on the diameter of the nanotubes, except possibly for the smallest diameters from 30 to 40 Å. The mechanical response of the nanotubes is highly nonlinear in the elastic regime, with the third-order elastic constant larger in zigzag nanotubes when compared with the armchair, and larger for the T nanotubes when compared with the H polytype. The defects have a negligible effect on Young's modulus, but the tensile strength decreases by a few GPa, and more importantly the nanotubes fracture in a brittle way at a considerable smaller strain. As expected, the defects including a W vacancy affect the point of rupture of the nanotubes more strongly than in the case that the defects where only a S atom is absent, but for any defect the fractures propagated following closely the circumference of the nanotube unlike the pristine nanotubes. It is believed that the marked differences in the mechanical properties of nanotubes of different polytypes could be important from a practical perspective, considering possible applications of WS_2 nanotubes where either easiness of deformation or fracture resistance are critical features for the use of these nanostructures.

Declaration of competing interest

The authors declare that they have no known competing financial interests or personal relationships that could have appeared to influence the work reported in this paper.

Acknowledgments

We wish to acknowledge J.A. de la Rosa for helping with the installation of the GPU card used in the simulation runs. Financial support from UANL, grants PAICYT CE1156-20 and CE1650-21, is also acknowledged.

References

[1] R. Tenne, L. Margulis, M. Genut, G. Hodes, Nature 360 (1992) 444.
[2] R. Rosentsveig, A. Margolin, Y. Feldman, R. Popovitz-Biro, R. Tenne, Chem. Mater. 14 (2002) 471.
[3] I. Kaplan-Ashiri, R. Tenne, JOM 68 (2016) 151.
[4] Z. Liu, A. Murphy, C. Kuppe, D.C. Hooper, V.K. Valev, A. Ilie, ACS Nano 13 (2019) 3896.
[5] I. Kaplan-Ashiri, S.R. Cohen, K. Gartsman, V. Ivanovskaya, T. Heine, G. Seifert, I. Wiesel, H.D. Wagner, R. Tenne, Proc. Natl. Acad. Sci. Unit. States Am. 103 (2006) 523.
[6] I. Kaplan-Ashiri, S.R. Cohen, K. Gartsman, R. Rosentsveig, G. Seifert, R. Tenne, J. Mater. Res. 19 (2004) 454.
[7] S. Deng, L. Li, M. Li, Phys. E Low-dimens. Syst. Nanostruct. 101 (2018) 44.
[8] A.N. Enyashin, L. Yadgarov, L. Houben, I. Popov, M. Weidenbach, R. Tenne, M. Bar-Sadan, G. Seifert, J. Phys. Chem. C 115 (2011) 24586.
[9] M.S. Sokolikova, C. Mattevi, Chem. Soc. Rev. 49 (2020) 3952.
[10] M. Damnjanović, T. Vuković, I. Milošević, Isr. J. Chem. 57 (2016) 450.
[11] S.J. Mejía-Rosales, S.A. Sandoval-Salazar, A. Soria-Sánchez, L.Y. Cantú-Sánchez, Mol. Simulat. 47 (2021) 471.
[12] F.H. Stillinger, T.A. Weber, Phys. Rev. B 31 (1985) 5262.
[13] J.-W. Jiang, Nanotechnology 26 (2015) 315706.
[14] J.-W. Jiang, Y.-P. Zhou, Parameterization of Stillinger-Weber Potential for Two-Dimensional Atomic Crystals, 2017 arXiv preprint arXiv:1704.03147.
[15] S. Plimpton, J. Comput. Phys. 117 (1995) 1.
[16] W.M. Brown, P. Wang, S.J. Plimpton, A.N. Tharrington, Comput. Phys. Commun. 182 (2011) 898.
[17] D. Kilymis, C. Gérard, J. Amodeo, U.V. Waghmare, L. Pizzagalli, Acta Mater. 158 (2018) 155.
[18] D. Çakır, F.M. Peeters, C. Sevik, Appl. Phys. Lett. 104 (2014) 203110.
[19] I. Kaplan-Ashiri, S.R. Cohen, K. Gartsman, R. Rosentsveig, V. Ivanovskaya, T. Heine, G. Seifert, H.D. Wagner, R. Tenne, Mater. Sci. Forum 475–479 (2005) 4097.
[20] D.-M. Tang, X. Wei, M.-S. Wang, N. Kawamoto, Y. Bando, C. Zhi, M. Mitome, A. Zak, R. Tenne, D. Golberg, Nano Lett. 13 (2013) 1034.
[21] K. Liu, Q. Yan, M. Chen, W. Fan, Y. Sun, J. Suh, D. Fu, S. Lee, J. Zhou, S. Tongay, J. Ji, J.B. Neaton, J. Wu, Nano Lett. 14 (2014) 5097.
[22] I.K. Ashiri, S.R. Cohen, V. Rosentsveig, V. Ivanovskaya, T. Heine, G. Seifert, H.D. Wagner, R. Tenne, AIP Conf. Proc. 723 (2004) 306.
[23] M.F. Ashby, Acta Metall. 37 (1989) 1273.
[24] G. Lopez-Polin, C. Gomez-Navarro, V. Parente, F. Guinea, M.I. Katsnelson, F. Perez-Murano, J. Gomez-Herrero, Nat. Phys. 11 (2014) 26.
[25] A.G. Kvashnin, P.B. Sorokin, D.G. Kvashnin, Fullerenes, Nanotub. Carbon Nanostruct. 18 (2010) 497.